Triangular Ising antiferromagnet: Boundary conditions, ground state entropy, and vortices

R. P. Millane* and R. M. Clare
Computational Imaging Group, Department of Electrical and Computer Engineering, University of Canterbury, Private Bag 4800, Christchurch, New Zealand

(Received 5 May 2005; revised manuscript received 27 August 2006; published 1 November 2006)

The ground state entropy density of the triangular Ising antiferromagnet is considered as a function of boundary conditions on domains for which the ground states do not admit a dimer covering. These domains admit a rich set of ground states that cannot be classified in the usual way in terms of nonintersecting strings. Various parametrized boundary conditions and domain shapes are identified that allow the ground state entropy density to be varied between zero and maximal degeneracy. The dependence of degeneracy on boundary spins and/or domain shape is interpreted in terms of strings that are not restricted to be nonintersecting.

DOI: 10.1103/PhysRevE.74.051101 PACS number(s): 05.50.+q, 75.10.Hk

I. INTRODUCTION

Frustrated systems do not order at zero temperature, have a highly degenerate ground state, and have application in a variety of physical systems [1–8]. It is well known that for some frustrated systems the infinite volume limit of the ground state entropy density of finite volume ensembles depends on the boundary condition of the finite system [9,10]. This is particularly interesting because the length of the boundary vanishes relative to the system size in the thermodynamic limit. The apparent paradox this raises was resolved by Aizenman and Lieb [10] who showed that the thermodynamic entropy density is the maximum over all boundary conditions. Except in a few cases, however, little is known about the general relationship between boundary conditions and ground state entropy.

The classical triangular Ising antiferromagnet (TIA) is an archetypical frustrated system for which the thermodynamic ground state entropy density depends exquisitly on the boundary conditions for finite volume ensembles [10–12]. However, the only case which is well understood is the rectangular domain with periodic boundary conditions, where the ground states admit a dimer covering and can be mapped to nonintersecting strings [13]. We recently identified a different class of boundary conditions that has a richer manifold of ground states that do not admit a dimer covering, and showed that the entropy density could be varied between zero and maximal degeneracy [12]. However, aside from identifying this class of boundary conditions, that work provided little fundamental insight into the relationship between boundary conditions and degeneracy. Here we extend this work in three ways. (1) We identify a larger class of boundary conditions on a triangular domain that give variable degeneracy, (2) we identify a variety of domain shapes whose *shape* controls the degeneracy, and (3) we show how the relationship between degeneracy and boundary conditions or domain shape can be interpreted in terms of strings that are not restricted to be nonintersecting. These results provide considerably more insight into this rich set of ground states.

*Electronic address: rick@elec.canterbury.ac.nz

II. BOUNDARY CONDITIONS AND ENTROPY DENSITY

The classical, isotropic TIA with nearest neighbor interactions has a thermodynamic ground state entropy density of ~ 0.3231 [14,15]. (The reader is alerted to the fact that the incorrect value of 0.3383 given in Ref. [14] has propagated quite widely in the literature.) We therefore define the normalised entropy density at absolute zero for a finite system of N spins with boundary condition B, $S_0(N,B)$, by

$$S_0(N,B) = \frac{\ln W(N,B)}{0.3231N}, \tag{1}$$

where $W(N,B)$ is the number of ground state configurations. Our interest here is in the thermodynamic limit

$$S_0(B) = \lim_{N\to\infty} S_0(N,B) \tag{2}$$

as a function of boundary condition.

A manifold of ground states that has been well characterised is the rectangular domain with periodic boundary conditions [13]. The ground states on this domain can be mapped to a dimer covering on the dual (hexagonal) lattice, which allows each ground state to be mapped to a configuration of nonintersecting strings [16]. In the thermodynamic limit the normalized entropy density, denoted by $\alpha(p)$, is a function of the string density (number of strings divided by the number of sites in a row) p, and is given by [13]

$$S_0(\mathrm{RP}(p)) = \alpha(p) = \frac{1}{0.3231}\left(p\ln 2 + \frac{2}{\pi}\int_0^{\pi p/2} \ln[\cos(x)]dx \right), \tag{3}$$

where $\mathrm{RP}(p)$ denotes a rectangular periodic boundary condition with string density p. The entropy density is zero for $p=0$ and $p=1$, and peaks at unity (maximal degeneracy) for $p=2/3$. Strings intersect the two opposite edges of the domain between each pair of adjacent opposite spins so that the string density can be calculated for a particular boundary condition, and the thermodynamic entropy density calculated by Eq. (3).

Only a restricted set of boundary conditions admit a dimer covering, however [16], and a richer manifold of ground states can be obtained from boundary conditions that do not

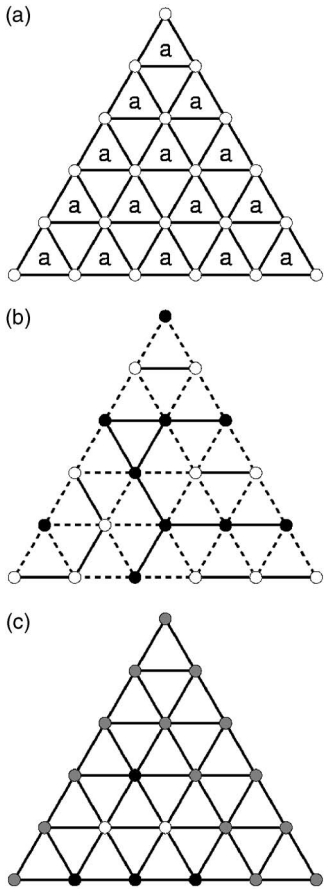

FIG. 1. (a) The triangular domain with the independent triangles labeled "a." (b) A ground state configuration with a high energy elementary triangle. Filled and open circles denote up and down spins, respectively, and favorable and unfavorable interactions are denoted by broken and solid lines, respectively. (c) Triangular domain with a triangular subdomain of fixed spins as described in the text. Gray circles denote free spins.

belong to this set. In particular, we identify here a wide variety of such boundary conditions that generate "partial degeneracy."

A dimer covering is possible only for ground states for which every elementary triangle is minimum energy (contains two opposite spins). This is the case for all ground states of the rectangular periodic domain. However, for the ground states on a finite triangular domain it is sufficient that the independent triangles labelled "a" in Fig. 1(a) are minimum energy [12]. The other elementary triangles may or may not be minimum energy. Therefore, the ground states on a finite triangular domain do not necessarily admit a dimer covering. An example of such a ground state is shown in Fig. 1(b). The high energy elementary triangles correspond to vortices if the ground states are mapped onto the solid-on-solid model [17].

In the following two sections we calculate the ground state entropy density for a variety of boundary conditions and domain shapes that do not admit a dimer covering. The entropy density was calculated by finite size scaling as described in Ref. [12] using an algorithm [18] that counts exactly the number of ground states.

III. ENTROPY DENSITY AS A FUNCTION OF BOUNDARY SPINS

In this section we derive some properties of the triangular domain and identify a parameterization of boundary spins that controls the entropy density. Although all "a" triangles being minimum energy is a sufficient condition for a ground state, it is a necessary condition only if such a configuration is consistent with the particular boundary condition being considered. Consider a boundary condition consisting of alternating spins on two edges and any configuration of fixed spins on the third edge. The spins on the row adjacent to the third edge can be chosen such that all the enclosed "a" triangles are minimum energy, and the process continued to the opposite vertex. The above condition is therefore necessary and sufficient for a ground state, and this is the class of boundary conditions we consider here.

Any configuration of fixed spins on the third edge can be partitioned into subsets, each subset containing either identical or alternating spins. Therefore, for a ground state, any triangular subdomain adjacent to a subset of identical spins must have spins fixed as shown in Fig. 1(c). If the total number of these fixed spins is N', the number of degrees of freedom of the system is reduced from N to $N-N'$. To study the thermodynamic entropy density on the triangular domain, N' must vanish relative to N in the limit, i.e., the boundary condition must satisfy

$$N'/N \to 0 \quad \text{as } N \to \infty . \tag{4}$$

If Eq. (4) is not satisfied, the domain size and shape, and the entropy density normalization, must be adjusted accordingly.

We note that the particular boundary condition on a triangular domain used in Ref. [12] does not satisfy Eq. (4), and the normalization used there is therefore incorrect. This resulted in entropy density values that are too small and a misleading comparison of the triangular domain with the rectangular periodic domain. The correct use of this boundary condition is described in Sec. IV of this paper.

To study the entropy density on the triangular domain we use here boundary conditions on the third edge that are a repeating finite pattern of spins and allow the number of repeats to go to infinity, so that N'/N is $O(N^{-1/2})$ and Eq. (4) is satisfied. For the rectangular periodic domain the entropy density is determined by the string density, which is equal to the density of pairs of adjacent opposite spins on the boundary. We therefore choose here sets of boundary conditions for the triangular domain that are parameterised by the density of pairs of adjacent opposite spins, and we denote this density by β. We generated boundary conditions with different patterns of spins with the same value of β, and for a variety of values of β. The boundary conditions are classified into six different patterns of spins which are labeled T1–T6, and these are listed in Table I together with the corresponding values of β. The thermodynamic entropy density for each value of β in each class was calculated as described above, and the results are listed in Table I and plotted versus β, using different symbols for each class, in Fig. 2(a). Note that the entropy density is independent of the class of the boundary condition, i.e., is a function of only β, and is denoted

TABLE I. Boundary conditions T1–T6 with the corresponding values of β and S_0.

Class	Repeating pattern	β	S_0
T1	OXO	2/3	1.01
	OXOO	1/2	0.94
	OXOOO	2/5	0.84
	OXOOOO	1/3	0.76
	OXOOOOO	2/7	0.69
	OXOOOOOO	1/4	0.63
T2	OXOXO	4/5	1.01
	OXOXOO	2/3	1.00
	OXOXOOO	4/7	0.97
	OXOXOOO	1/2	0.93
T3	OXOXOXO	6/7	1.01
	OXOXOXOO	3/4	1.00
T4	OXXO	1/2	0.94
	OXXOO	2/5	0.84
	OXXOOO	1/3	0.76
	OXXOOOO	2/7	0.66
	OXXOOOOO	1/4	0.62
T5	OXXXOO	1/3	0.76
	OXXXOOO	2/7	0.68
	OXXXOOOO	1/4	0.62
T6	OXXXXOOO	1/4	0.62

$S_0(\mathrm{T}(\beta))$. A third order polynomial fit to the data $S_0(\mathrm{T}(\beta))$ is shown as the solid line in Fig. 2(a). The entropy density for the rectangular periodic domain $\alpha(\beta)$ (since $p=\beta$ for this domain), is shown for comparison as the dashed line in Fig. 2(a). The results in Fig. 2(a) are discussed in Sec. V.

IV. ENTROPY DENSITY AS A FUNCTION OF DOMAIN SHAPE

In this section we identify various polygonal domains with fixed boundary spins for which the entropy density is controlled by the *shape* of the domain. These domains are generated by starting with a triangular domain and choosing boundary conditions that do not satisfy Eq. (4). The triangular subdomains referred to in Sec. III then grow with the domain size and are excluded from the system, thus modifying the shape of the domain. The entropy density for the modified domain is then calculated by appropriate normalization. We consider three such examples.

Consider first a triangular domain with n spins on each edge, alternating spins on two of the edges, γn contiguous alternating spins at one end of the third edge $(0<\gamma<1)$ and the remaining spins identical [Fig. 3(a)]. (Note that this is the boundary condition considered, but incorrectly interpreted, in Ref. [12].) The fraction of spins in the triangular subdomain is then finite and the boundary condition generates a trapezium domain with relative edge lengths $\{1,\gamma,(1-\gamma),\gamma\}$ with all boundary spins alternating, which is denoted $\mathrm{P1}(\gamma)$ [Fig. 3(b)]. The parameter γ controls the shape of the domain; for $\gamma=1$ it is triangular and for $0<\gamma<1$ it is a trapezium with aspect ratio proportional to $1/\gamma$. The entropy density $S_0(\mathrm{P1}(\gamma))$ was computed for various values of γ and the results are shown in Fig. 2(b). A third order polynomial fit to the data is shown by the curve in the figure. The behavior of $S_0(\mathrm{P1}(\gamma))$ as $\gamma\to 0$ is not clear so the curve is not extended to $\gamma=0$.

Consider second a triangular domain with alternating spins on two edges, γn contiguous alternating spins at the center of the third edge, and the remaining spins identical as shown in Fig. 3(c). This boundary condition generates a pentagon domain with relative edge lengths $\{(1+\gamma)/2,(1-\gamma)/2,\gamma,(1-\gamma)/2,(1+\gamma)/2\}$ and all boundary spins alternating as shown in Fig. 3(d). This domain is denoted $\mathrm{P2}(\gamma)$ and γ controls the shape of the domain. The length of the bottom edge in Fig. 3(c) is proportional to γ, and the domain approaches a rhombus for $\gamma\to 0$ and a triangle for $\gamma\to 1$. The entropy density for this domain $S_0(\mathrm{P2}(\gamma))$ was calculated and is plotted as a function of γ in Fig. 2(b).

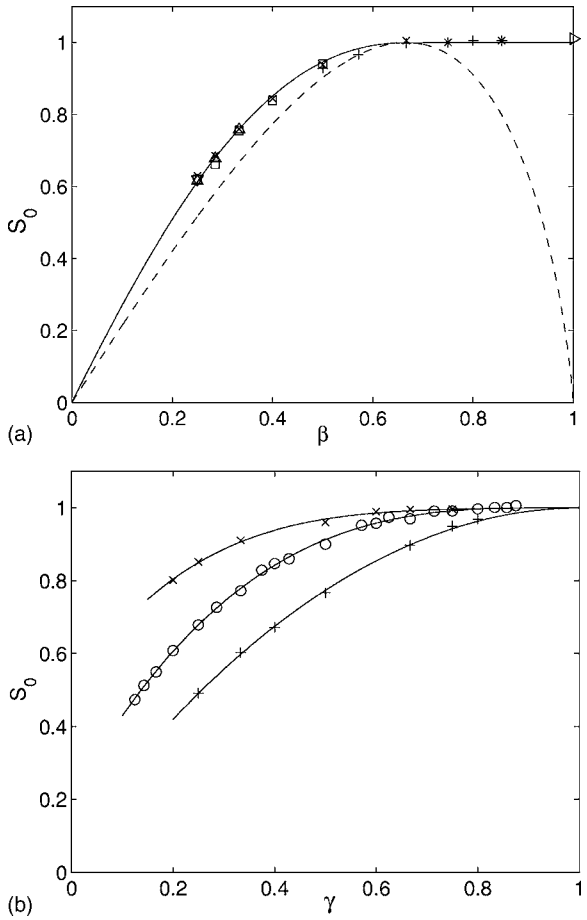

FIG. 2. (a) Normalized entropy densities for boundary conditions T1–T6 (each represented by a different symbol) versus β. The solid curve shows a third order polynomial fit to all the data $S_0(\mathrm{T}(\beta))$ for $0<\beta<2/3$ and $S_0(\mathrm{T}(\beta))=1$ for $2/3<\beta<1$. The dashed curve shows $\alpha(\beta)$. (b) Normalized entropy densities $S_0(\mathrm{P1}(\gamma))$ (o), $S_0(\mathrm{P2}(\gamma))$ (×), and $S_0(\mathrm{P3}(\gamma))$ (+) versus β. Third order polynomial fits are shown by the solid lines.

Third, consider a triangular domain with alternating spins on two edges, $(1-\gamma)n$ contiguous identical spins at the center of the third edge and the remaining spins alternating as shown in Fig. 3(e). This boundary condition generates a hexagon domain with relative edge lengths $\{1,\gamma/2,(1-\gamma),(1-\gamma),\gamma/2,1\}$ and all boundary spins alternating as shown in Fig. 3(f). This domain is denoted P3(γ) and has the shape of an inverted V with the widths of the two "legs" proportional to $\gamma/2$. The entropy density $S_0(\mathrm{P3}(\gamma))$ was calculated and is shown as a function of γ in Fig. 2(b).

The polygon domains P1(γ), P2(γ), and P3(γ) with fixed boundary spins are therefore examples for which the entropy density varies as a function of the *shape* of the domain. The results in Fig. 2(b) are discussed in the next section.

V. DISCUSSION

For boundary conditions whose ground states admit a dimer covering (e.g., for a rectangular periodic domain) the entropy density can be calculated using a classification in terms of conserved, nonintersecting strings [13]. The boundary conditions described in this paper admit a richer manifold of ground states in which high energy "non-a" triangles (vortices) are not frozen out. The ground states can be mapped onto strings, but the strings are neither nonintersecting nor conserved on rows. Two strings coalesce at each vortex [e.g., Fig. 4(a)], reducing the number of strings at the next row by 2.

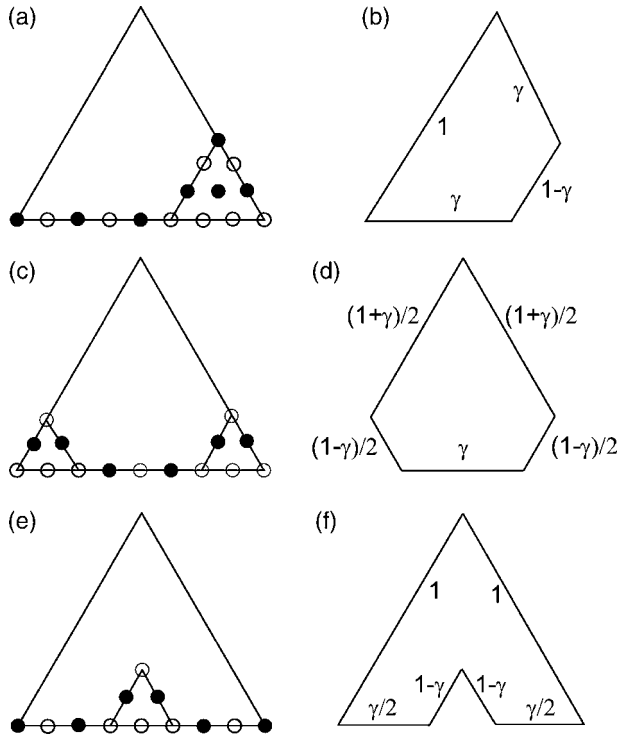

FIG. 3. (a), (c), and (e) Boundary conditions on a triangular domain showing triangles with fixed spins in the ground state. Open and closed circles represent up and down spins, respectively. The generated polygon domains (b) P1(β), (d) P2(β), and (f) P3(β), with alternating boundary spins and relative edge lengths as shown.

For the case of a triangular domain, the parameter β is equal to the density of strings that intersect the bottom edge. Referring to Fig. 2(a), the two primary observations are that $S_0(\mathrm{T}(\beta))\geq\alpha(\beta)$ for all β, and that $S_0(\mathrm{T}(\beta))=1$ for $\beta>2/3$, whereas $\alpha(\beta)$ is a decreasing function of β for $\beta>2/3$. These two observations can be understood as follows. For the triangular domain, additional string configurations, over those for the rectangular peroidic domain, are accessible by the formation of vortices, resulting in a larger entropy density on the former domain. The entropy density on both domains increases as the string density increases, since more strings gives more configurations, until $\beta=2/3$ where the number of configurations is a maximum and the entropy density reaches its bulk value. As β increases beyond 2/3, for the rectangular periodic domain the strings become more tightly packed (since they are nonintersecting and conserved) and the number of accessible configurations reduces, until at $\beta=1$ the strings are completely packed and there is only one configuration. For the triangular domain however, as β increases beyond 2/3, although the strings are more tightly packed on the bottom edge, the system exploits (a) configu-

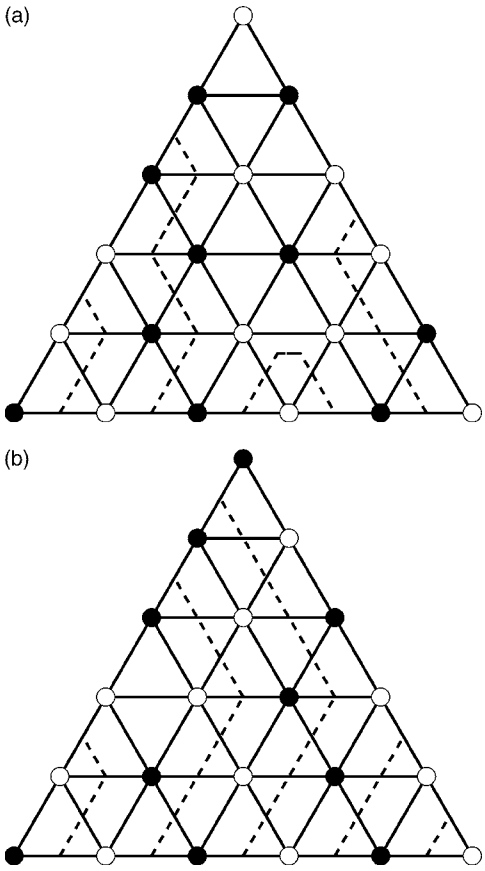

FIG. 4. Minimum energy configurations with the strings shown by dashed lines in which (a) two strings form a vortex and (b) two strings exit the domain at the same row.

rations containing vortices and (b) configurations where two strings exit the domain at one row, that reduce the string density on the higher rows. This allows more configurational freedom (since $\beta > 2/3$) and maximal degeneracy is maintained up to $\beta = 1$. Examples are shown in Fig. 4. In Fig. 4(a) a vortex between the first and second rows reduces the string density from 1 to 3/4. In Fig. 4(b) two strings exit above the second row and the string density reduces from 1 to 2/3. If the strings are evenly distributed on the bottom edge in the limit of large N (as they are for the boundary conditions used here) then the number of string configurations, and thence the entropy density is determined by the string density β on the bottom edge. In contrast to the rectangular periodic domain, the string density is variable on the other rows.

For the case of the polygon domains with alternating boundary spins, referring to Fig. 2(b), the two primary observations are that the entropy density is an increasing function of γ for all γ, and that

$$S_0(\mathrm{P2}(\gamma)) > S_0(\mathrm{P1}(\gamma)) > S_0(\mathrm{P3}(\gamma)). \tag{5}$$

The string density on the bottom edge of the domains is unity and a finite entropy density results from the presence of vortices and strings exiting the sides of the domain as described above for the triangular domain. The variation in entropy density is due to the number of string configurations allowed by the boundary shape (which is controlled by γ). Referring to Fig. 3, for domains P1 and P3 decreasing γ increases the number of rows relative to the number of strings. Since strings may coalesce or exit the domain, the effect is that for smaller γ there tends to be fewer strings on higher rows, and hence fewer total configurations, and the entropy density decreases. For the domain P2, the domain shape changes from a rhombus (for which the system is nondegenerate [11]) at $\gamma = 0$ to a triangle at $\gamma = 1$ for which the system is maximally degenerate. The relationship (5) can be understood by considering the range of string configurations accessible for the different boundary shapes as follows. The strings can adopt more configurations the more they can "spread out" without leaving the domain. Maximum spreading can occur if the strings at each end of the lower edge can be oriented at 30° *away* from the bisector of the edge. Referring to Fig. 3 shows that this is the case for domain P2 but not for domains P1 and P3, so that the entropy density is largest for domain P2. For domains P1 and P3 the orientations of the edges adjoining the bottom edge(s) is the same, however, for domain P3 the two narrow "legs" increase the probability of strings leaving the domain, thus reducing the total number of configurations and the entropy density, for domain P3 compared to domain P1.

In summary, we have presented examples of boundary conditions for the TIA that admit a richer manifold of ground states than those that admit a dimer covering. We have identified parametrizations of these boundary conditions that allow the entropy density to be varied between nondegenerate and maximal degeneracy. The ground states can contain vortices, which for boundary conditions that admit a dimer covering are characteristic only of excited states. The entropy density on these domains is determined by the number of configurations of strings that are neither nonintersecting nor conserved. For the triangular domain the entropy density is a function of the string density on the bottom edge (the only row on which it is fixed for a particular boundary condition). For the polygon domains the number of string configurations, and thence the entropy density, is determined by the shape, and properties such as the aspect ratio, of the domain.

ACKNOWLEDGMENT

We are grateful to the NZ Marsden Fund for financial support.

[1] R. Liebmann, *Statistical Mechanics of Periodic Frustrated Ising Systems* (Springer-Verlag, Berlin, 1986).
[2] B. Simon, *The Statistical Mechanics of Lattice Gases* (Princeton University Press, Princeton, 1993), Vol. 1.
[3] G. Aeppli and P. Chandra, Science **275**, 177 (1997).
[4] D. Davidović, S. Kumar, D. H. Reich, J. Siegel, S. B. Field, R. C. Tiberio, R. Hey, and K. Ploog, Phys. Rev. B **55**, 6518 (1997).
[5] R. Moessner and S. L. Sondhi, Phys. Rev. B **63**, 224401 (2001).
[6] A. P. Ramirez, Nature (London) **421**, 483 (2003).
[7] M. Mezard, Science **301**, 1685 (2003).
[8] R. F. Wang, C. Nisoli, R. S. Freitas, J. Li, W. McConville, B. J. Cooley, M. S. Lund, N. Samarth, C. Leighton, V. H. Crespi, and P. Schiffer, Nature (London) **439**, 303 (2006).
[9] R. B. Griffiths, J. Math. Phys. **6**, 1447 (1965).
[10] M. Aizenman and E. H. Lieb, J. Stat. Phys. **24**, 279 (1981).
[11] R. P. Millane, A. Goyal, and R. C. Penney, Phys. Lett. A **311**, 347 (2003).
[12] R. P. Millane and N. D. Blakeley, Phys. Rev. E **70**, 057101 (2004).
[13] A. Dhar, P. Chaudhuri, and C. Dasgupta, Phys. Rev. B **61**, 6227 (2000).
[14] G. H. Wannier, Phys. Rev. **79**, 357 (1950).
[15] R. M. F. Houtappel, Physica (Amsterdam) **16**, 425 (1950).
[16] B. Nienhuis, H. J. Hilhorst, and H. W. J. Blöte, J. Phys. A **17**, 3559 (1984).
[17] H. W. J. Blöte and M. P. Nightingale, Phys. Rev. B **47**, 15046 (1993).
[18] N. D. Blakeley and R. P. Millane, Comput. Phys. Commun. **174**, 198 (2006).